GEOLOGICAL SURVEY OF CANADA
OPEN FILE 7617

Overview of the 2013 Baseline Magnetotelluric and Controlled-Source Electromagnetic Geophysical Study of CO_2 Sequestration at the Aquistore site near Estevan, Saskatchewan

J. McLeod, J.A. Craven, I.J. Ferguson, B.J. Roberts, B. Bancroft and T. Liveda

2014

Natural Resources Canada | Ressources naturelles Canada

Canada

GEOLOGICAL SURVEY OF CANADA
OPEN FILE 7617

Overview of the 2013 Baseline Magnetotelluric and Controlled-Source Electromagnetic Geophysical Study of CO_2 Sequestration at the Aquistore site near Estevan, Saskatchewan

J. McLeod[1], J.A. Craven[2], I.J. Ferguson[1], B.J. Roberts[2], B. Bancroft[2] and T. Liveda[3]

[1]University of Manitoba, Winnipeg, Manitoba
[2]Geological Survey of Canada, Ottawa, Ontario
[3]Memorial University, St. John's, Newfoundland and Labrador

2014

doi:10.4095/293921

This publication is available for free download through GEOSCAN (http://geoscan.nrcan.gc.ca/).

Recommended citation
McLeod, J., Craven, J.A., Ferguson, I.J., Roberts, B.J., Bancroft, B. and Liveda, T., 2014, Overview of the 2013 Baseline Magnetotelluric and Controlled-Source Electromagnetic Geophysical Study of CO_2 Sequestration at the Aquistore site near Estevan, Saskatchewan; Geological Survey of Canada, Open File 7617, 23 p., doi:10.4095/293921

Publications in this series have not been edited; they are released as submitted by the author.

Contents

Figures & Tables

Introduction

The Aquistore project is a large-scale carbon dioxide (CO_2) capture and sequestration initiative, taking place to the southwest of Estevan, Saskatchewan. Emissions of CO_2 generated from SaskPower's nearby Boundary Dam Power Station are to be captured and injected, in liquid form, deep into stable sedimentary packages of the Williston Basin for long-term storage (Aquistore, 2013). The overall aim of the project is to reduce greenhouse gas emissions coming from a fixed source of CO_2 discharge, while demonstrating the effectiveness of using geological formations as a sequestration reservoir (Whittaker and Worth, 2011). Carbon capture and storage (CCS), in combination with renewable energy technologies, is potentially a strong means of mitigating anthropogenic climate change.

The Aquistore reservoir will be the Cambro-Ordovician aquifer system of the Deadwood and Winnipeg Formations of the Williston basin which forms part of the Western Canada Sedimentary Basin (Aquistore 2013). The primary electromagnetic target is at 3400 m depth, which is deep in comparison to other CO_2 site studies. The reservoir at Ketzin is at 635-650 m depth, at Hontomín it is at 1350-1460 m, and at Kevin Dome it is at 3000 m. The Aquistore target lies beneath a thick sequence of very conductive (<10 Ω.m) rocks of the Jurassic to Paleocene Zuni succession (Jones 1988, Gowan et al., 2009). The surface environment in the study area includes a number of possible sources of electromagnetic noise including infrastructure of the Boundary Dam Power Station and Prairie farming operations. The electromagnetic noise may create challenges for both controlled source and natural source measurements (Ferguson, 2012; Escalas et al., 2013).

The project discussed herein focuses on surface controlled-source and natural source electromagnetic monitoring methods. These methods provide an economic complement or alternative to surface seismic monitoring methods in the monitoring of CO_2injection. They also eliminate the need for subsurface borehole access to deploy monitoring sensors. To date, relatively few such measurements have been made in association with CO_2 storage projects. Examples of sites at which surface electromagnetic methods have been applied or modelled include proposed CO_2 sites at Kevin Dome in the United States (Zhdanov et al., 2013), Ketzin in Germany (Streich et al., 2011) and Hontomín in Spain (Ogaya et al., 2013). Related studies have also been conducted at geothermal sites, e.g., the Paralana site in Australia (Peacock et al., 2013). In the future, feasibility modeling will be conducted to assess the sensitivity of surface electromagnetic measurements to the displacement of brine by CO_2, the dissolution of CO_2 within the brine in the reservoir, and leakage into the overlying strata. Time-lapse natural and controlled-source electromagnetic surveys will be conducted to monitor subsurface changes in electrical conductivity.

A component of the surface controlled-source electromagnetic investigations at Aquistore includes a survey by British Petroleum (BP) and GroundMetrics, Inc. (GMI) using a novel borehole to surface electromagnetic (BSEM) survey configuration (Hibbs, 2013). This method injects an electric current using a surface array of electrodes oriented radially to the well. Measurement at the surface of the distribution of electric current that return from reservoir depths via the injection well casing provides a means to detect signals from reservoir depths.

Overview of the Aquistore Project

Prior to being released into the atmosphere, the waste gases created the Boundary Dam power station will be treated with an amine solvent to remove CO_2. The CO_2 is then dehydrated and compressed for transportation and storage, while the solvent undergoes a heating and cooling cycle that allows it to be reused (Gibbins and Chalmers, 2008). Captured carbon products will be transported to the injection well via pipeline. Of an anticipated 3,000 tons of CO_2 captured by SaskPower each day, 2,000 tons are destined for geological storage. The remaining CO_2 will be sold to Cenovus Energy for the purposes of enhanced oil recovery (Aquistore, 2013; SaskPower, 2013).

A number of factors make the Winnipeg and Deadwood formations in the Williston Basin ideal targets for CO_2 sequestration. This section of the sedimentary sequence consists of porous rock, capable of storing vast amounts of injected fluid. At depths greater than 3 km, these formations lie beneath the region's oil reservoirs and potash-bearing rocks, and have no economic value themselves (Aquistore, 2013). Impermeable layers seal the reservoir from potential leakage. The tectonically stable setting of the Williston Basin is also an important aspect for the long-term storage goals (Aquistore, 2013).

A crucial part of the project is monitoring of the subsurface response to the injected fluid. The continued injection of CO_2 will be dependent on the integrity of the sealing units and on the subsurface distribution of the fluid. A suite of monitoring techniques are being utilised at the Aquistore site to ensure that these requirements are being satisfied at multiple stages of the injection (Aquistore, 2013).

The intent of the NRCan Integrated CO_2 Measurement, Monitoring & Verification Study is to simultaneously test and calibrate monitoring tools (other than seismics) at the CO_2 injection site. 3D time-lapse seismic methods have been the predominant monitoring tool utilized in pilot CO_2 injection/storage projects. Other less intensive monitoring methods are desirable to either complement or substitute for seismic methods. Ultimately, the observations will be quantitatively integrated to estimate the subsurface distribution of CO_2 and ground deformation that may affect the integrity of the storage complex. From this comprehensive monitoring suite, a minimum set of tools can be tailored to achieve the required goals in future monitoring programs.

As a subset of Aquistore's monitoring program, this research will employ electromagnetic (EM) techniques to provide time-lapse mapping of the CO_2 plume. Magnetotelluric (MT) and controlled-source electromagnetic (CSEM) data collected at the Aquistore site will be used to produce images of the changing electrical properties of the storage complex as the CO_2 is being injected. Natural and controlled-source electromagnetic monitoring of electrical conductivity at sub-surface injection and extraction sites can provide valuable constraints on changes in fluid content and fluid salinity. We seek to test if characteristic electrical resistivity signature in images derived from the MT and CSEM data will serve as a proxy for the concentration and spatial distribution of CO_2. At Aquistore, seismic surveys will predominate in the characterisation of the evolving reservoir (Aquistore, 2013). The

extent to which EM methods could be a source of complementary information to the existing time-lapse seismic methods will also be assessed over the life of the NRCan study.

Geological Setting

Williston Basin

The Williston Basin is a large intracratonic sedimentary basin that extends from southern Saskatchewan and southwest Manitoba into Montana and South Dakota (Figure 1). The basin lies unconformably overtop of a basement of Archean and Proterozoic-aged cratons (Fowler and Nisbet, 1984). In east-central Saskatchewan, the basin thickness is between 2.2 and 3 km (Whittaker and Worth, 2011). Ages of the constituent strata range from middle Cambrian to early Cenozoic. Continuous subsidence from the Cambrian to the Jurassic is suggested as the driving mechanism of the Williston Basin's development (Fowler and Nisbet, 1884). The subsidence following the Jurassic is noted to be more complex and influenced by tectonic forces to the west. Alternatively, Zhu and Hajnal (1993) propose nine distinct episodes of subsidence interpreted from seismic data.

Figure 1. Aerial extent of the Williston Basin (Whittaker and Worth, 2011).

The Basin's sedimentary record is notably incomplete. Unconformities from periods of erosion and non-deposition correlate well with changes in sea level (Figure 2) (Fowler and Nisbet, 1984). The deepest rocks of the basin are the sandstones of the Deadwood Formation, which are separated from the Precambrian rocks below, and the Middle Ordovician Winnipeg formation above by erosional unconformities. The Winnipeg Formation consists of sandstone and shale, and is a part of the Tippecanoe sequence (Binda and Simpson, 1989). Carbonates, evaporites and shale characterize the overlying Kaskaskia sequence. The Triassic shales of the succeeding Lower Watrous Formation are unconformably overlain by the Jurassic evaporites of the Upper Watrous. This sequence lies beneath

the Zuni sequence and surficial glacial deposits of the Pleistocene (Gowan et al., 2009). Collectively, the strata of the Williston Basin form alternating sequences of aquifers and aquitards (Figure 3).

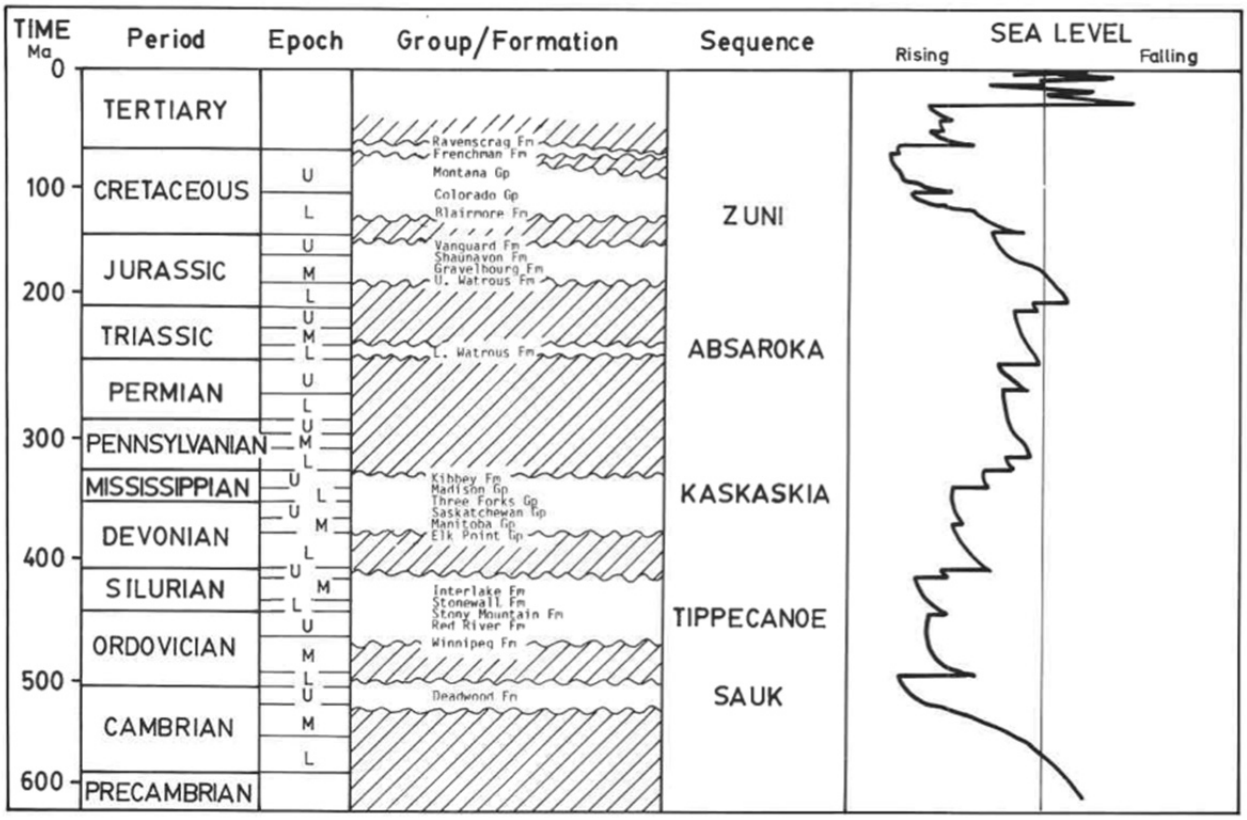

Figure 2. Regional stratigraphy of the Williston Basin in Saskatchewan (Fowler and Nisbet, 1984).

Deadwood Formation

The Cambro-Ordovician Deadwood formation lies unconformably overtop of the Precambrian basement, and is the basal unit of the Williston Basin in the study area. Moving west, the unit thickens rapidly, and is underlain by the Earlie Formation and Basal Sandstone unit (Maclean, 1960; Dixon, 2008). In the eastern portion of the Williston Basin, the Deadwood Formation is predominantly a sandstone layer, whereas in Alberta, the formation consists mostly of shales. Sandstones of the northern Deadwood Formation are highly glauconitic. The sandstones become more quartzose and generally coarser grained to the south (Maclean, 1960). Interbeds of silty and shaly rocks in the Deadwood add heterogeneity to the unit (Whittaker and Worth, 2011). The beds of the formation show an upward coarsening character (Dixon, 2008).

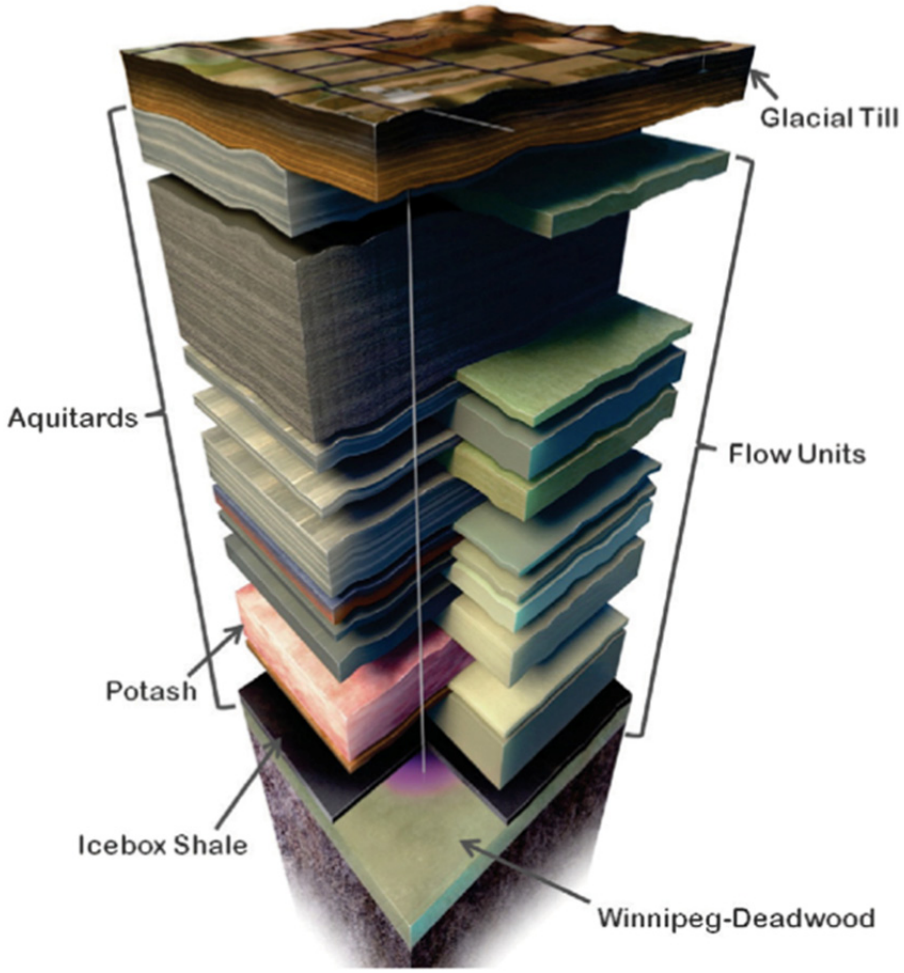

Figure 3. Hydrostratigraphy of the Williston Basin at the Aquistore site (Whittaker and Worth, 2011).

Winnipeg Formation

The Winnipeg Formation is predominantly a sandstone aquifer, deposited in the Middle to Late Ordovician following early subsidence in the Williston Basin (Smith and Bend, 2004). The sequence lies unconformably overtop of the Cambrian to Lower Ordovician Deadwood Formation, and near the edges of the Williston Basin, the Precambrian basement (Figure 4). In North Dakota, the sequence reaches a maximum thickness of over 100 m (Binda and Simpson, 1989).

Subdivisions of the formation include the Black Island, Icebox and Roughlock members (Smith and Bend, 2004; Ferguson et al., 2007). The Black Island package is the lowest member in the formation and consists of well to poorly-sorted quartzose sandstone. The Black Island sandstones are differentiated from the Deadwood Formation by a higher textural and mineralogical maturity, an absence of glauconite, and lower gamma-ray log radioactivity counts (Binda and Simpson, 1989). Lying conformably overtop of the Black Island sandstones are the shales of the Icebox member. These shales have been interpreted as an extensive flooding surface (Smith and Bend, 2004). The Roughlock member is the uppermost subunit of the Winnipeg Formation. Where present, the Roughlock provides a smooth transition from the Icebox member to the overlying carbonates of the Upper Ordovician Red

River Formation. However, the Icebox member is not present in most of Saskatchewan, and in these areas, the contact between the Red River and Winnipeg formations is unconformable (Smith and Bend, 2004). At the Aquistore site, the Icebox member will serve as the primary seal for the injected fluid (Whittaker and Worth, 2011).

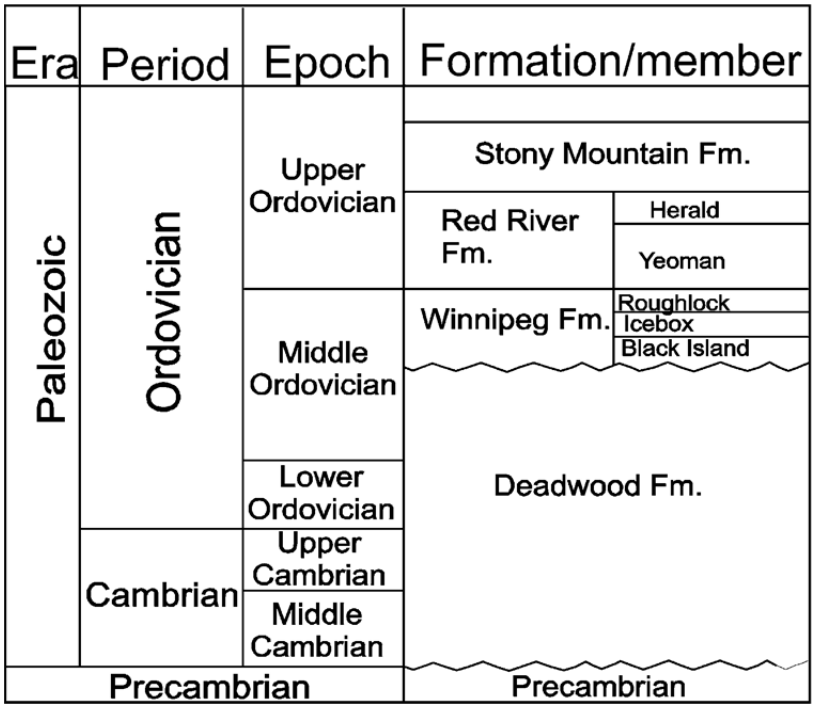

Figure 4. Stratigraphic section of the lower Williston Basin (Smith and Bend, 2004).

Background Electromagnetic Theory

Previous Synthetic and Field EM Studies of CO_2 Sequestration

Electromagnetic geophysical techniques detect variation in the electrical resistivity of the subsurface materials and fluids. A number of petrophysical models numerically quantify the relationship between pore fluid resistivity and the resistivity that can be inferred from an EM study. These models are based on various factors including pore geometries, clay content and interconnectivity and salinity of the pore fluid. Due to density contrasts, it is expected that CO_2 and brine will largely separate in the reservoir (Huang et al., 2014). In a lab experiment, Fleury and Deschamps (2008) found that as CO_2 was introduced to a saline solution, the resistivity changed according to the following simple function of temperature (T, ^{o}C) and molar fraction of CO_2 (x_{CO_2}):

$$\rho(x_{CO_2}, T) = \left[\rho(x_{CO_2}, T_o)(1 - 6.0x_{CO_2})\left(\frac{T + 19.5}{T - 19.5}\right)\right]^{-1} \quad (1)$$

Incorporation of equation (5) into a simple petrophysical model from Archie (1942) results in resistivity dependant on molar fraction CO_2 and a range of reservoir porosities (Figure 5). The implication is that methods to detect a temporal change in electrical resistivity at depth will image a

temporal change in the mole fraction of CO_2 within the aquifer, under the condition that all else remaining constant. As the injection proceeds CSEM should, in theory, be able to detect the spatial progression of the plume away from the injection well; and may be able to detect leakage through overlying aquitards if the experiment is designed to explore at the proper range of depths.

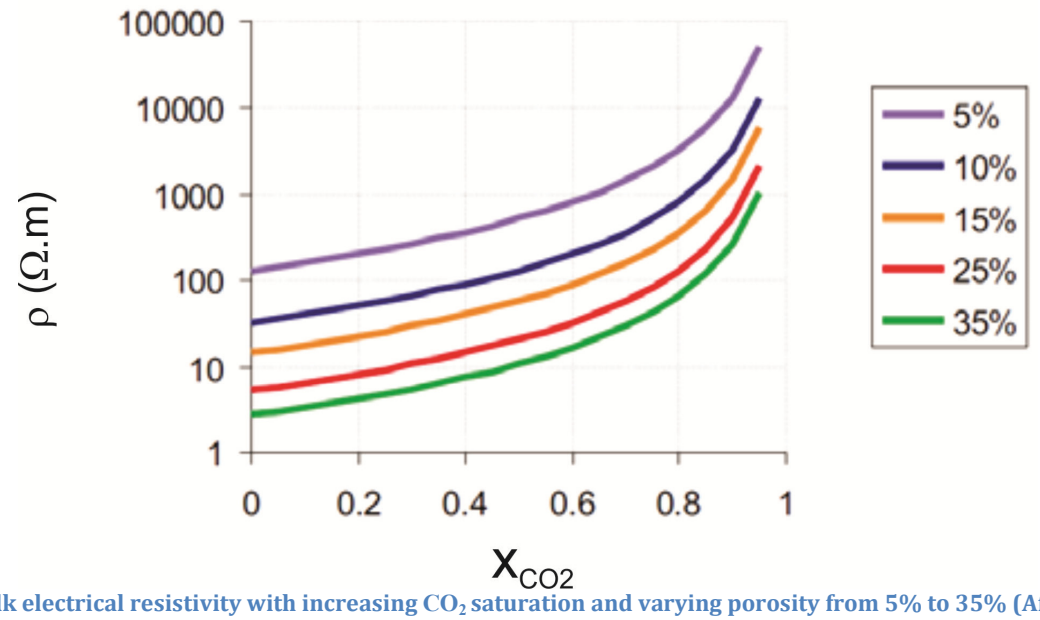

Figure 5. Bulk electrical resistivity with increasing CO_2 saturation and varying porosity from 5% to 35% (After Jones, 2013).

MT and controlled-source methods have previously been used to characterize CO_2 storage complexes in Hotomin, Spain and Ketzin, Germany. At the Hotomin site, pre-injection studies indicate that the contrast in electrical resistivity of the reservoir rock and the primary seal is sufficient to identify any changes in the rock properties following an injection (Ogaya, et al., 2013). It is anticipated that the CO_2 will introduce a detectable high resistivity signature to the host aquifer (Vilamajo et al., 2012). Numerical modelling of the feasibility of detecting CO_2 plumes near Ketzin using CSEM methods offer mixed results. Streich et al. (2010) conclude that CO_2 may be clearly identified using EM methods, but that not all source-receiver configurations provide the resolution needed to observe growth of the plume over time. Vertical electric field sensors placed in boreholes would be ideal for CO_2 detection.

The MT Method

The MT method relies on naturally occurring geomagnetic variations to induce electric currents in the Earth's subsurface. It therefore has the advantage of not requiring the costly and time consuming deployment of a man-made controlled source of EM energy. Orthogonal components of the secondary magnetic and electric fields arising naturally from the currents are recorded as time series at the surface. The underlying geoelectric structure may then be inferred from the relationships between these field components (see for example Vozoff, 1991; Simpson and Bahr, 2005).

Horizontal electric and magnetic field components are related by the impedance tensor, $\boldsymbol{Z}$:

$$\begin{pmatrix} E_x \\ E_y \end{pmatrix} = \begin{pmatrix} Z_{xx} & Z_{xy} \\ Z_{yx} & Z_{yy} \end{pmatrix} \begin{pmatrix} H_x \\ H_y \end{pmatrix} \tag{2}$$

The significance of the impedance tensor is its description of the dimensionality and strike of the subsurface resistivity structure. The impedance elements are determined using auto- and crosspowers of the frequency-domain field components. The solutions often will also include remote referenced data (Gamble et al., 1979) to minimize local noise on magnetic field components. It is convenient to express the impedance magnitude in terms of the apparent resistivity as:

$$\rho_{a,ij}(\omega) = \frac{1}{\mu_0 \omega} \left| Z_{ij}(\omega) \right|^2 \tag{3}$$

The phase is given by:

$$\varphi_{ij}(\omega) = \tan^{-1}\left(\frac{\mathrm{Im}\{Z_{ij}\}}{\mathrm{Re}\{Z_{ij}\}} \right) \tag{4}$$

The relationship between the vertical magnetic field component and the horizontal magnetic field components is given by the tipper function, $\boldsymbol{T} = [T_x, T_y]$ where:

$$H_z = T_x H_x + T_y H_y \tag{5}$$

Both the tipper and the impedance tensor are complex. Induction arrows are the vector representation of tipper functions. These arrows may be used to identify lateral conductivity gradients as vertical magnetic fields are produced by these variations.

The different types of geoelectric structure that might be encountered are: 1D, where resistivity varies only with depth; 2D, where resistivity varies with depth and one horizontal direction; and 3D, where resistivity varies in all spatial directions. The 1D and 2D (for a coordinate system aligned with geoelectric strike) scenarios will produce characteristic impedance tensors (Vozoff, 1991; Simpson and Bahr, 2005). The EM signals in 2D structure are commonly separated into TE (current flow is parallel to the strike) and TM (current flow is perpendicular to strike) modes. Knowing the strike and dimensionality of the subsurface structure will permit informed choices of inversion methods, and superior models of the subsurface resistivity structure. It is the subsurface resistivity structure which is altered by the injection of the CO_2 as discussed later.

Although relatively inexpensive and comparatively easy to deploy, an MT survey is unlikely to be sensitive to a thin resistor (i.e. the CO_2) at a depth of 3400m due to the inherent lack of sensitivity of inductive EM techniques to such features. Inductive techniques rely primarily on the generation of eddy currents within conductive material to provide a detectable signal that can be used to infer subsurface properties. Nonetheless, MT can provide an estimate of the background (i.e. regional) electrical structure associated with the Williston Basin and the underlying basement and constrain uncertainties in the analysis of other datasets sensitive to similar rock properties. To provide direct detection of thin resistors at depth resulting from CO_2 injection it is advisable to use CSEM methods as they inject a current vertically and the resulting spatial current distributions and electric fields will be noticeably affected upon encountering the resistive layer.

Controlled-Source Electromagnetism

Controlled source EM geophysical exploration has undergone a resurgence primarily within the marine oil & gas industry. One of the proven advantages of the marine CSEM technique is its ability to detect thin resistive layers at considerable depths (e.g. Johansen et al., 2005). It has been also been shown that the imaged resistivity of the thin layer correlates reasonably well with the oil saturation within the layer. In a typical marine CSEM project a dipole transmitter is lowered off a ship to a point close to the seabed and receivers are deployed on the seafloor in a profile behind the ship. In such a configuration it is possible to explore for thin resistors (using low frequency sources) at depths of over 4 km depending on local conditions. To a large extent, the key anomalous response to detect the thin layer is exhibited in the component of the electric field parallel and in-line the transmitter bipole. Given the resistivities in a terrestrial sedimentary basin are not unlike those in a marine environment, it is not unreasonable to expect CSEM techniques on land with an acquisition geometry comparable to the marine setup to be able to detect a thin resistive feature related to CO_2injection. Gasperikova and Hoversten (2006) have indeed demonstrated that terrestrial CSEM techniques can be sensitive to CO_2 content of layers > 1km in depth and to movement of the fluids within the layer (Figure 6) of the order 500m. A portion of the anomalous response, *i.e.* the positive change in Figure 6b, is located at the proper position; however the negative changes are offset from the proper location. Only through modelling and inversion can one properly locate and determine spatial resolution of the feature (Zhadnov et al., 2013). We will present more detailed numerical calculations of expected responses in a later paper. The primary purpose of this open file is to document the 2013 field experiments.

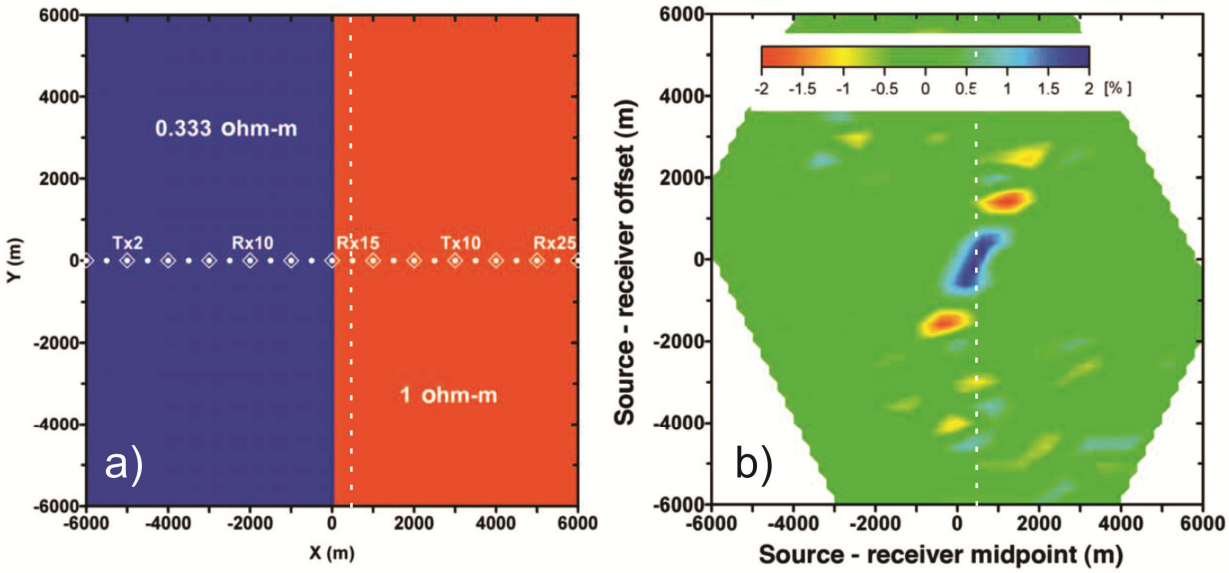

Figure 6. a) Plan view of a highly simplified reservoir resistivity model with a fluid layer at 1200m depth consisting of saline fluids (blue) and CO_2 rich fluids (red). Tx (diamonds) and Rx (small squares) signify bipole and receiver locations, respectively. b) Percent change in the inline electric field amplitudes for various offsets and source receiver midpoints if the contact is shifted 500m to the east (dashed lines). Modified from Gasperikova and Hoversten (2006).

NRCan EM studies at Aquistore

The MT and CSEM sites recorded in 2013 are shown in Figure 7 and summarized in Table 2 & 2. A few of the sites sampled both MT and CSEM data. Site 02 was situated distant to the survey area (~10 km) to facilitate special computations to reduce noise in the MT and CSEM response calculations. E-field sensors at each site recorded perpendicular horizontal components at each MT/CSEM site, but only in-line components were recorded at the long offset CSEM sites. A variety of sampling rates and soundings were utilized to facilitate either or both MT and CSEM calculations at sites. Magnetic sensors were installed as indicated in Table 2. Site 02 was sounded by GroundMetrics Inc. independently after completion of our work in order to develop algorithms to predict and remove telluric noise during CSEM surveys.

In general, night time recordings are preferable to be used to calculate the MT response due to the enhanced natural signal. Calculation of the daytime MT response is possible, but one must be careful to exclude time periods when the CSEM transmitter is active. Difficulties in processing the data at sites 01 and 07 resulted in having to move to nearby locations (sites 05 and 13 respectively). The noise source at site 01 could be related to distortion in the local current systems due to the nearby steel-cased injection and monitoring wells. The noise source at site 07 may be related to solar powered electric fences <100 m from the site. The pattern of MT sites was selected in order to be able to discern an expected largely radially uniform spatial response of the subsurface pressures to the injection (Whittaker and Worth, 2011).

The surface transmitter for the CSEM study performed at the Aquistore site was configured as a horizontal electric bipole (grounding points shown in Figure 7). The transmitter waveform of the bipole was an alternating square-wave energized at range of frequencies. In the frequency domain the harmonics of the square waves can also be utilized to determine responses. Where available, the complementary magnetic field measurements will provide additional constraints on the level of anisotropy and degree of heterogeneity in the survey area. In contrast to the MT survey, the CSEM survey was set up largely in a single profile running SW-NE due to the limited receiver equipment and personnel to perform a larger experiment. The profile azimuth was chosen in order to align with the regional fluid flow in this portion of the Basin (Bachu and Hitchon, 1996) as it is expected that it will have a small influence on the radial outward progression of the injected fluids. In addition, we expect our MT measurements collected simultaneous to the CSEM survey will serve to mitigate the influence of natural noise in the CSEM data. The background telluric noise may hamper the detection of weak man-made signals from deep reservoirs that unfortunately are comparable to the background signals.

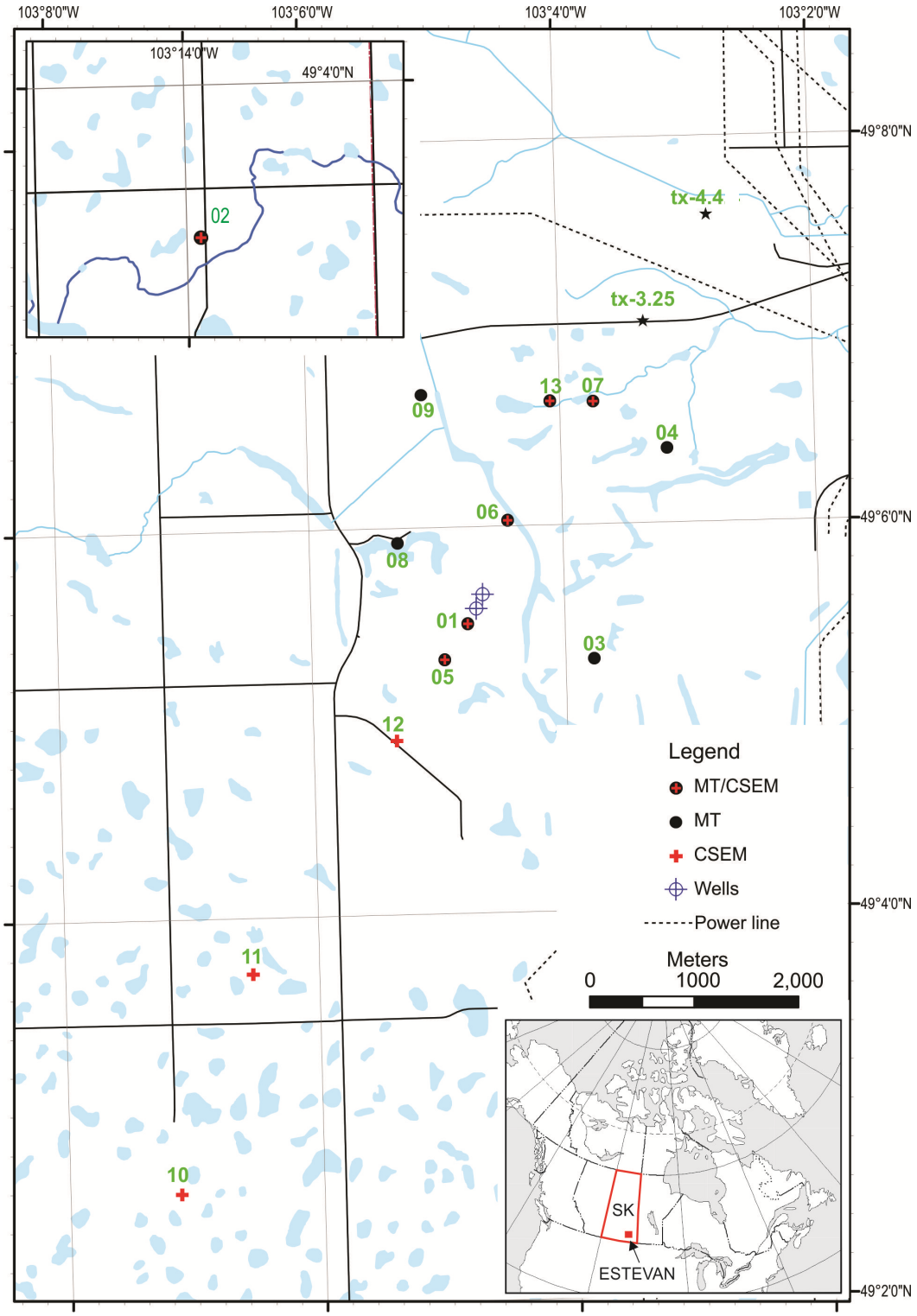

Figure 7. 2013 Aquistore MT and CSEM sites. Grounding points of bipole transmitter shown with black stars and labels (tx-3.25 and tx-4.4) in terms of distance (3.25 and 4.4 km respectively) from the injection well. Site 02 is located about 10 km west of the other sites and is used as the remote reference site to reduce contribution of noise to the MT and CSEM sites.

Current & Future Work

Currently, we are completing an analysis of an existing regional MT data set (Jones, 1982) to provide a basin-scale picture of the background resistivity structure. Analysis of new MT time series, including separating the controlled-source from the passive-source data, is also underway with the overarching goal of the calculation of robust, low-noise, CSEM and MT responses. In addition to the data analysis, numerical modelling of the source fields produced by the transmitter for a range of injection simulations and theoretical multidimensional modelling of MT responses associated with CO_2 injection are also underway.

Future field work will also entail the collection of similar datasets during and post-injection (i.e. during extraction) in order to determine if a signature within the responses or images is directly attributable to injection of CO_2. It is possible that a signature in MT responses may reflect or map the injection, but due to the physics underlying MT may not be used to infer or resolve subsurface information such as mole-fraction CO_2. A signature that may resolve mole-fraction CO_2 could arise in time lapse CSEM datasets.

Acknowledgements

Without the capable help of GroundMetrics Inc. running the transmitter for us, the CSEM study could not have been completed. Bernard Giroux at INRS is thanked for loan of his MTUs and transmitter. The local farmers are kindly thanked for providing permission to use their land. SaskPower provided us space on site to stage gear and charge batteries. Lisa Roach provided comments and suggestions that have enhanced this report.

References

Aquistore, 2013, Aquistore web page. http://aquistore.ca/, accessed 02 August 2013.

Archie, G., 1942, The electrical resistivity log as an aid in determining some reservoir characteristics: Transactions of the American Institute of Mechanical Engineers, 146, 54–62.

Asten, M., 1988. The downhole magnetometric resistivity (DHMMR) method. Explor. Geophys., 19, 2, 12-16.

Bachu, S. and B. Hitchon. 1996. Regional-Scale Flow of Formation Waters in the Williston Basin, AAPG Bull., V.80, No. 2, pp. 248-264.

Bishop, J., Lewis, R. & Stolz, N., 2000. Horses for (conductive) courses: DHEM and DHMMR. Explor. Geophys., 31, 192-199.

Binda, P.L. and Simpson, E.L. (1989): Petrography of sulphide-coated grains from the Ordovician Winnipeg Formation, Saskatchewan, Canada; *European Journal of Mineralogy*, Volume 1, pages 439-453.

Dixon, J. (2008): Stratigraphy and facies of Cambrian to Lower Ordovician strata in Saskatchewan; *Bulletin of Canadian Petroleum Geology*, Volume 56, pages 93-117.

Edwards, R.N., & Nabighian, N.M. (1991): The magnetometric resistivity method. Chapter 2, in *Electromagnetic Methods in Applied Geophysics, Volume 2, Applications,* ed. M.N. Nabighian, Society of Exploration Geophysicists, Tulsa, p. 47- 104.

Ferguson, A.G., Betcher, R.N., and Grasby, S.E. (2007): Hydrogeology of the Winnipeg Formation in Manitoba, Canada; *Hydrogeology Journal*, Volume 15, pages 573-587.

Fleury, M. and Deschamps, H., 2008, Electrical Conductivity and Viscosity of Aqueous NaCl Solutions with Dissolved CO_2, J. Chem. Eng. Data, 2008, 53 (11), pp 2505–2509, DOI: 10.1021/je800262

Fowler, C.M.R. and Nisbet, E.G, 1984, The subsidence of the Williston Basin; *Canadian Journal of Earth Sciences*, Volume 22, pages 408-415.

Gamble, TD, WM Goubeau, and J. Clarke (1979), Magnetotellurics with a remote reference, Geophysics, 44, 53–68, doi:10.1190/1.1440923

Gasperikova, E., and G. M. Hoversten, 2006, A feasibility study of nonseismic geophysical methods for monitoring geologic CO_2 sequestration: The Leading Edge, 25, 1282–1288, doi: 10.1190/1.2360621.

Gibbins, J. and Chalmers, H., 2008, Carbon Capture and Storage; *Energy Policy*, Volume 36, pages 4317-4322.

Gowan, E.J., Ferguson, I.J., Jones, A.G., and Craven, J.A., 2009, Geoelectric structure of the northeastern Williston basin and underlying Precambrian lithosphere; *Canadian Journal of Earth Sciences*, Volume 46, pages 441-464.

Hibbs, A., 2013, Test of a new BSEM configuration at Aquistore, and its application to mapping injected CO_2, June 26, 2013. BP project Task 1 report, 7 pp.

Huang, X., Bandilla, K.W., Celia, M. A., and Bachu, S., 2014, Basin-scale modeling of CO_2 storage using models of varying complexity, *International Journal of Greenhouse Gas Control,* 20, 73-86.

Johansen, S.E., Amundsen, H.E.F., Røsten, T., Ellingsrud, S., Eidesmo, T., and Bhuyian, A.H., 2005, Subsurface hydrocarbons detected by electromagnetic sounding: first break, 23, 31-36.

Jones, A.G., 1993, The COPROD2 dataset: Tectonic setting, recorded MT data, and comparison of models; *Journal of Geomagnetism and Geoelectricity*, Volume 45, pages 933-955.

Jones, A.G., 2013, IRECCSEM: Evaluating Ireland's potential for onshore carbon sequestration and storage using electromagnetics, http://www.ireccsem.ie/overview.html

McLean, D.D., 1960, Deadwood and Winnipeg stratigraphy in east-central Saskatchewan; *Saskatchewan Department of Mineral Resources-Sedimentary Geology Division*, Report no. 47, 35 pages.

Ogaya, X., Ledo, J., Queralt, P., Marcuello, A., and Quinta, A., 2013, First geoelectric image of the subsurface of the Hontomin site (Spain) for CO_2 geological storage: A magnetotelluric 2D characterization; *International Journal of Greenhouse Gas Control*, Volume 13, pages 168-179.

SaskPower, 2013, SaskPower web page http://www.saskpower.com/, accessed 20 October 2013.

Simpson, F. and Bahr, K., 2005, Practical Magnetotellurics. Cambridge University Press, United Kingdom.

Smith, M. and Bend, S., 2004, Geochemical analysis and familial association of Red River and Winnipeg reservoired oils of the Williston Basin, Canada; *Organic Geochemistry*, Volume 35, pages 443-452.

Streich, R., Becken, M., and Ritter, O., 2010, Imaging of CO_2 storage sites, geothermal reservoirs, and gas shales using controlled source magnetotellurics: Modeling studies; *Chemie der Erde*, Volume 70, pages 63-75.

Vozoff, K. (1991): The magnetotelluric method. In: Nabighian, M.N. (Ed.), Electromagnetic Methods in Applied Geophysics – Volume 2 Applications. Society of Exploration Geophysicists, Tulsa, pages 641-711.

Ward, S.H & Hohmann, G.W., 1988, Electromagnetic Theory for Geophysical Applications; Chapter 4 in *Electromagnetic Methods in Applied Geophysics, Vol. I, Theory,* ed. Nabighian, M.N, Soc. Exploration Geophysicists, Tulsa, Okla, p. 131-311.

West, G.F. & Macnae, J.C., 1991, Physics of the electromagnetic induction exploration method. *Chapter 1 in* Electromagnetic Methods in Applied Geophysics, Volume 2, Part A, *edited by* Nabighian, M.N., Society of Exploration Geophysicists, Tulsa, OK, USA, pages 5-45.

Whittaker, S. and Worth, K., 2011, Aquistore: a fully integrated demonstration of the capture, transportation and geologic storage of CO_2; *Energy Procedia*, Volume 4, pages 5607-5614.

Zhdanov, M.S., Endo, M., Black, N., Spangler, L., Fairweather, S., Hibbs, A., Eiskamp, G.A., and Will, R., 2013, Electromagnetic monitoring of CO_2 sequestration in deep reservoirs; *First Break*, Volume 31, pages 71-78.

Zhu, C. and Hajnal, Z., 1993, Tectonic development of the northern Williston basin: a seismic interpretation of an east-west regional profile; *Canadian Journal of Earth Sciences*, Volume 30, pages 621-630.

Table 1 NRCan 2013 MT and CSEM Receiver and Transmitter Locations

Tx-3.25	N49.11761	W103.05547
Tx-4.4	N49.12668	W103.04685
Aqi001	N49.09178	W103.07950
Aqi002	N49.05358	W103.23127
Aqi003	N49.08853	W103.06299
Aqi004	N49.10656	W103.05274
Aqi005	N49.08872	W103.08262
Aqi006	N49.10062	W103.07393
Aqi007	N49.11070	W103.06233
Aqi008	N49.09887	W103.08844
Aqi009	N49.11160	W103.08489
Aqi010	N49.04314	W103.11885
Aqi011	N49.06194	W103.10882
Aqi012	N49.08180	W103.08915
Aqi013	N49.11081	W103.06800

Table 2. 2013 MT and CSEM Acquisition Paremeters

Data File	Start	Site	Coils	E-line Anchor Spacing	Azimuth of x Direction	Ex Line Length (m)	Ey Line Length (m)	Notes
15628LAA	2013-08-21	aqi002	HX: MT8C7320, HY:MT8C7319, HZ: none	none	0 MN	nil	nil	ACQ=MT
28588LAA	2013-08-21	aqi004	none	1-2m	0 MN	46.1	47.2	ACQ=MT
28598LAB	2013-08-21	aqi005	none	none	0 MN	50	50	ACQ=MT
28608LAB	2013-08-21	aqi003	Hx: MT8C8051 Hy: MT8C7322, HZ: none	1-2m	0 MN	50	50	ACQ=MT
1561821A	2013-08-21	aqi001	Hx: MT8C8052 Hy: MT8C8053, HZ: none	1-2m	0 MN	50	50	ACQ=MT will only process using local coils cannot import these coils to other sites
2861821A	2013-08-21	aqi006	none	1-2m	0 MN	49	47	ACQ=MT
1562822A	2013-08-22	aqi002	HX: MT8C7320, HY:MT8C7319, HZ: none	none	0 MN	nil	nil	ACQ=MT
2858822A	2013-08-22	aqi004	HX:AMTC1170 HY: AMTC1171, HZ: none	1-2m	0 MN	46.1	47.2	ACQ=AMT
2859822A	2013-08-22	aqi005	HX:AMTC1173 HY: AMTC1174, HZ: none	none	0 MN	50	50	ACQ=AMT
2860822A	2013-08-22	aqi003	Hx: MT8C8051 Hy: MT8C7322, HZ: none	1-2m	0 MN	50	50	ACQ=MT
1561822A	2013-08-22	aqi001	Hx: MT8C8052 Hy: MT8C8053, HZ: none	1-2m	0 MN	50	50	ACQ=AMT E-lines (N,E,W) disturbed by ATVs; battery and MTU toppled when lines pulled
2861822A	2013-08-22	aqi006	none	1-2m	0 MN	49	47	ACQ=AMT
1562823A	2013-08-23	aqi002	HX: MT8C7320, HY:MT8C7319, HZ: none	none	0 MN	nil	nil	ACQ=AMT, LEV2=0 (so effectively MT with continuous 150 Hz)
2858823A	2013-08-23	aqi007	none	1-2m	0 MN	50.9	53	ACQ=AMT, LEV2=0 (so effectively MT with continuous 150 Hz) poor long period data: due to solar powered electric fence nearby?
2859823A	2013-08-23	aqi005	HX:AMTC1173 HY: AMTC1174, HZ: none	none	0 MN	50	50	ACQ=AMT, LEV2=0 (so effectively MT with continuous 150 Hz)

2860823A	2013-08-23	aqi001	Hx: MT8C8052 Hy: MT8C8053, HZ: none	1-2m	0 MN	50	50	ACQ=AMT, LEV2=0 (so effectively MT with continuous 150 Hz) - coils cannot be imported as local coils and likely cannot be used as remote coils
1561823A	2013-08-23	aqi003	Hx: MT8C8051 Hy: MT8C7322, HZ: none	1-2m	0 MN	50	50	ACQ=AMT, LEV2=0 (so effectively MT with continuous 150 Hz)
2861823A	2013-08-23	aqi006	none	1-2m	0 MN	49	47	ACQ=AMT, LEV2=0 (so effectively MT with continuous 150 Hz)
1562824A	2013-08-24	aqi002	HX: MT8C7320, HY:MT8C7319, HZ: none	none	0 MN	nil	nil	ACQ=AMT, LEV2=1 (so a little AMT, with continuous 150 Hz)
2858824A	2013-08-24	aqi007	none	1-2m	0 MN	50.9	53	ACQ=AMT, LEV2=1 (so a little AMT, with continuous 150 Hz) (better than run 'a', but not much)
2859824A	2013-08-24	aqi005	HX:AMTC1173 HY: AMTC1174, HZ: none	none	0 MN	50	50	ACQ=AMT, LEV2=1 (so a little AMT, with continuous 150 Hz)
2860824A	2013-08-24	aqi001	Hx: MT8C8052 Hy: MT8C8053, HZ: none	1-2m	0 MN	50	50	ACQ=AMT, LEV2=1 (so a little AMT, with continuous 150 Hz) daytime only (for CSEM)
1561824A	2013-08-24	aqi008	HX:AMTC1216 HY: AMTC1172, HZ: none	3 m	0 MN	51.1	50.2	ACQ=AMT, LEV2=1 (so a little AMT, with continuous 150 Hz) night only
2861824A	2013-08-24	aqi006	none	1-2m	0 MN	49	47	ACQ=AMT, LEV2=1 (so a little AMT, with continuous 150 Hz)
2860824B	2013-08-24	aqi009	Hx: MT8C8051 Hy: MT8C7322, HZ: none	3 m	0 MN	59	58.9	ACQ=AMT, LEV2=1 (so a little AMT, with continuous 150 Hz) night only
1464825A	2013-08-25	aqi002	HX: MT8C7320, HY:MT8C7319, HZ: none	none	0 MN	nil	nil	*continuous 15 Hz for GMI afternoon CSEM recordings* *MTU 1562 unable to start; overheating suspected*
2858825A	2013-08-25	aqi007	none	1-2m	0 MN	50.9	53	ACQ=AMT, LEV2=1 (so a little AMT, with continuous 150 Hz)
2859825A	2013-08-25	aqi005	HX:AMTC1173 HY: AMTC1174, HZ: none	none	0 MN	50	50	ACQ=AMT, LEV2=1 (so a little AMT, with continuous 150 Hz) mtu and E eline disturbed by cattle but no breaks
1561825B	2013-08-25	aqi008	HX:AMTC1216 HY: AMTC1172, HZ: none	3 m	0 MN	51.1	50.2	ACQ=AMT, LEV2=1 (so a little AMT, with continuous 150 Hz) night only
2861825A	2013-08-25	aqi006	none	1-2m	0 MN	49	47	ACQ=AMT, LEV2=0 (so effectively MT with continuous 150 Hz) daytime recording only for CSEM

1561825A	2013-08-25	aqi001	none	1-2m	0 MN	50	50	ACQ=AMT, LEV2=1 (so a little AMT, with continuous 150 Hz) daytime only (for CSEM)
2860825A	2013-08-25	aqi009	Hx: MT8C8051 Hy: MT8C7322, HZ: none	3 m	0 MN	59	58.9	ACQ=AMT, LEV2=1 (so a little AMT, with continuous 150 Hz)
2861825B	2013-08-25	aqi002	HX: MT8C7320, HY:MT8C7319, HZ: none	none	0 MN	nil	nil	ACQ=AMT, LEV2=1 (so a little AMT, with continuous 150 Hz)
1561826A	2013-08-26	aqi003	none	1-2m	0 MN	50	50	ACQ=AMT, LEV2=1 (so a little AMT, with continuous 150 Hz)
1562826A	2013-08-26	aqi004	HX:AMTC1170 HY: AMTC1171, HZ: none	1-2m	0 MN	46.1	47.2	ACQ=AMT, LEV2=1 (so a little AMT, with continuous 150 Hz)
2859826A	2013-08-26	aqi005	HX:AMTC1173 HY: AMTC1174, HZ: none	none	0 MN	50	50	ACQ=AMT, LEV2=1 (so a little AMT, with continuous 150 Hz)
2860826A	2013-08-26	aqi009	Hx: MT8C8051 Hy: MT8C7322, HZ: none	3 m	0 MN	59	58.9	ACQ=AMT, LEV2=1 (so a little AMT, with continuous 150 Hz)
2861826A	2013-08-26	aqi002	HX: MT8C7320, HY:MT8C7319, HZ: none	none	0 MN	nil	nil	*ACQ=AMT, LEV2=1 (so a little AMT, with continuous 150 Hz) coil leads severed*
2858826B	2013-08-26	aqi013	none	none	0 MN	51.2	51.7	ACQ=AMT, LEV2=1 (so a little AMT, with continuous 150 Hz) sometimes referred to as 007alt
2861827A	2013-08-27	aqi002	HX: MT8C7320, HY:MT8C7319, HZ: none	none	0 MN	nil	nil	daytime CSEM (but no transmission I believe) ACQ=AMT, LEV2=0 (so effectively MT with continuous 150 Hz)
1561827A	2013-08-27	aqi010	none	none	22 MN	49.4	nil	daytime CSEM (but no transmission I believe) ACQ=AMT, LEV2=0 (so effectively MT with continuous 150 Hz)
2859827A	2013-08-27	aqi011	none	none	22 MN	50.4	nil	daytime CSEM (but no transmission I believe) ACQ=AMT, LEV2=0 (so effectively MT with continuous 150 Hz)
2860827A	2013-08-27	aqi012	none	none	22 MN	50.7	nil	daytime CSEM (but no transmission I believe) ACQ=AMT, LEV2=0 (so effectively MT with continuous 150 Hz)
2861828A	2013-08-28	aqi002	HX: MT8C7320, HY:MT8C7319, HZ: none	none	0 MN	50.4	51.2	ACQ=AMT, LEV2=0 (so effectively MT with continuous 150 Hz) can be used to process MT
1561828A	2013-08-28	aqi010	none	none	22 MN	49.4	nil	daytime CSEM ACQ=AMT, LEV2=0 (so effectively MT with continuous 150 Hz)

2859828A	2013-08-28	aqi011	none	none	22 MN	50.4	nil	daytime CSEM ACQ=AMT, LEV2=0 (so effectively MT with continuous 150 Hz)
2860828A	2013-08-28	aqi012	none	none	22 MN	50.7	nil	daytime CSEM ACQ=AMT, LEV2=0 (so effectively MT with continuous 150 Hz)
GMI-remoteonly-data								
2861828A	2013-08-28	aqi002	HX: MT8C7320, HY:MT8C7319, HZ: none	none	0 MN	nil	nil	ACQ=AMT, LEV2=0 (so effectively MT with continuous 150 Hz)
2861829A	2013-08-29	aqi002	HX: MT8C7320, HY:MT8C7319, HZ: none	none	0 MN	nil	nil	ACQ=AMT, LEV2=0 (so effectively MT with continuous 150 Hz)
2861829B	2013-08-29	aqi002	HX: MT8C7320, HY:MT8C7319, HZ: none	none	0 MN	nil	nil	ACQ=AMT, LEV2=0 (so effectively MT with continuous 150 Hz)
2861830A	2013-08-30	aqi002	HX: MT8C7320, HY:MT8C7319, HZ: none	none	0 MN	nil	nil	ACQ=AMT, LEV2=0 (so effectively MT with continuous 150 Hz)
2861831A	2013-08-31	aqi002	HX: MT8C7320, HY:MT8C7319, HZ: none	none	0 MN	nil	nil	ACQ=AMT, LEV2=0 (so effectively MT with continuous 150 Hz)
2861901A	2013-09-01	aqi002	HX: MT8C7320, HY:MT8C7319, HZ: none	none	0 MN	nil	nil	ACQ=AMT, LEV2=0 (so effectively MT with continuous 150 Hz)
2861902A	2013-09-02	aqi002	HX: MT8C7320, HY:MT8C7319, HZ: none	none	0 MN	nil	nil	ACQ=AMT, LEV2=0 (so effectively MT with continuous 150 Hz)